

Minimum Race-Time Planning-Strategy for an Autonomous Electric Racecar

Thomas Herrmann¹, Francesco Passigato¹, Johannes Betz¹ and Markus Lienkamp¹

Abstract—Increasing attention to autonomous passenger vehicles has also attracted interest in an autonomous racing series. Because of this, platforms such as Roborace and the Indy Autonomous Challenge are currently evolving. Electric racecars face the challenge of a limited amount of stored energy within their batteries. Furthermore, the thermodynamical influence of an all-electric powertrain on the race performance is crucial. Severe damage can occur to the powertrain components when thermally overstressed. In this work we present a race-time minimal control strategy deduced from an Optimal Control Problem (OCP) that is transcribed into a Nonlinear Problem (NLP). Its optimization variables stem from the driving dynamics as well as from a thermodynamical description of the electric powertrain. We deduce the necessary first-order Ordinary Differential Equations (ODE)s and form simplified loss models for the implementation within the numerical optimization. The significant influence of the powertrain behavior on the race strategy is shown.

I. INTRODUCTION

The first autonomous race series for all-electric racecars is called *Roborace*. Its main goal is to be a platform for the development of software powering self-driving cars. Therefore, Roborace is a race format, bringing cars to their limits of handling [1]. The special requirements for the algorithms regarding computational resources, real-time capability, and robustness are thus outstanding [2], [3]. The race format of autonomous motor-sports delivers perfect conditions for testing under tough conditions in an enclosed environment. We, a team from the Technical University of Munich (TUM), are participating in this race series. Most parts of our software stack are available online [4]. This paper describes the extension of our software by a control strategy calculating the minimum race-time, taking into account energetic and thermal constraints arising from the powertrain architecture. The minimum time control strategy is one of three parts of our race strategy (Fig. 1). As discussed in the results section of this paper, the powertrain thermodynamics have a major impact on the entire race strategy.

This paper is based on the ideas for an energy management strategy for autonomous electric cars as stated in our previous work [5]. We extend the state of the art by taking into account multiple race laps as well as the thermodynamics of the all-electric powertrain in the OCP that needs to be solved.

A. State of the Art

OCPs dealing with trajectory optimization, which is equivalent to solving a Minimum Lap Time Problem (MLTP) in motor-sports, are well known in the literature. Different mathematical approaches are used to solve an MLTP. The variety ranges from graph search methods [6] over Sequential Quadratic (SQP) [7] to Second Order Conic Problems (SOCP) [8]. By the transformation of the OCP into an NLP, the MLTP can be solved with detailed and complex double-track vehicle and tire models for the purpose of, e.g., vehicle parameter optimization for Internal Combustion Engine (ICE) powered cars [9]–[11]. Latest publications in the field of trajectory optimization also consider optimal power distributions within hybrid powertrains [12] or use Model Predictive Control (MPC)-approaches for the planning of energy-saving trajectories [13].

However, none of these sources consider the thermodynamics of the powertrain during their optimizations. Unless the temperature limits of a conventional ICE, the electric machines of the Roborace cars must not reach temperatures beyond 180 °C, the inverter's limit is 100 °C [14]. Additionally, the efficiency level of an electric machine decreases as it heats up, leading to further reduction in efficiency [15], [16]. Furthermore, the energy storage, a lithium-ion battery in our case, must reduce its output power from 50 °C to 0 % output power when reaching 55 °C for safety reasons [14]. In order to therefore prevent the unwanted power loss, the thermal behavior of the powertrain components must be considered for consecutive race laps when dealing with all-electric racecars.

This paper is organized as follows: In Subsection I-B, an overview of the structure of our race strategy is given. Section II describes the powertrain architecture including power loss descriptions, thermodynamical models as well as the formulation of the optimization problem. Section III explains the results in detail. A summary of the presented work is given in Section IV.

B. Structure of the race strategy

The race strategy is split into three levels. All of these levels have a different optimization horizon as well as a different problem size stemming from the combination of their optimization horizon as well as their model complexities (Fig. 1).

Before the race starts, the global time-minimal trajectories per lap for the entire race are calculated offline. Here, we can use a non-linear double track model describing the driving dynamics as well as a detailed thermal powertrain

¹Thomas Herrmann (corresponding author), Francesco Passigato, Johannes Betz and Markus Lienkamp are with the Chair of Automotive Technology, Faculty of Mechanical Engineering, Technical University of Munich, 85748 Garching (Munich), Germany thomas.herrmann@tum.de

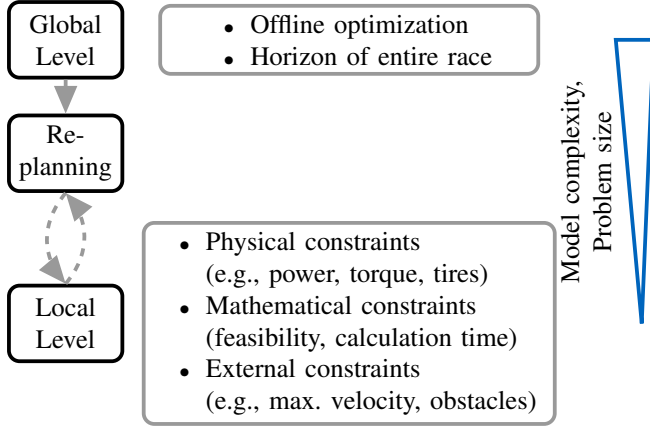


Fig. 1: Three levels of the proposed race strategy.

model to consider all necessary physical effects in detail. The pre-computed global trajectories are recalculated during the race, reacting to external disturbances, e.g., overtakes, using a significantly reduced optimization problem formulation. For example, the path can often be completely removed during the replanning phase as it is almost equal for all the race laps. The global trajectories are then fed into the local trajectory planner that transforms all given physical constraints from the global trajectory (e.g., max. power, max. torque) as well as mathematical requirements (e.g., guaranteed feasibility, calculation time) into locally optimal paths and velocities [17]. Furthermore, the local planner considers external influences, e.g., overtakes opponent cars or reacts to speed limits. In this paper we focus on the global level of the proposed race strategy and describe the offline optimization.

II. POWERTRAIN ARCHITECTURE & MODELING

The all-electric powertrain of the racecar (Fig. 2) consists of

- A battery (B).
- Two power electronics/inverters at rear left and right ($I_{l/r}$).
- Two synchronous permanent electric machines ($M_{l/r}$).

Two separate cooling circuits are necessary in order to control the component temperatures T_c . Circuit 1 is responsible for machines $M_{l/r}$ and inverters $I_{l/r}$ leveraging radiator R_{MI} . The same is true for circuit 2, battery B and radiator R_B . For the sake of completeness, the gears ($G_{l/r}$), sensors required for autonomous driving (A_x), as well as the wheels $W_{rr/rl}$, are also displayed within the rear part of the whole powertrain.

In this work, the index c indicates the powertrain component, i.e., $c \in \{M, I, B, R_{MI}, R_B\}$. The second index d of the temperature symbols of both cooling liquids $T_{F1/2,d}$ enumerates the components the fluids are entering.

A. Power loss models

Meta-models of the powertrain are used to describe the internal losses of its components within the OCP. Mathemat-

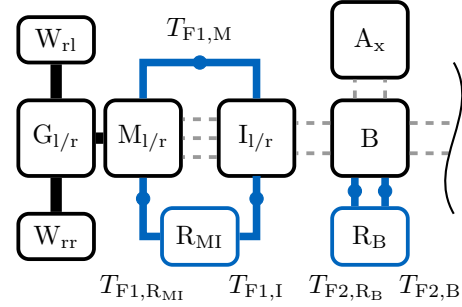


Fig. 2: Electric powertrain architecture of a rear-wheel drive vehicle including two separate cooling circuits.

ically, the meta-models for the electric machines as well as the inverters can be formulated as second order polynomials with the output power P_{out} as free variable (1):

$$P_{in,fit}(P_{out}) = a_{fit}P_{out}^2 + b_{fit}P_{out} + c_{fit}. \quad (1)$$

The Mean Square Error (MSE) $e_{MS,fit}$,

$$e_{MS,fit} = \frac{1}{N} \sum_i^N (P_{in,fit,i} - P_{in,mes,i})^2 \quad (2)$$

is minimized by fitting the constant parameters a_{fit} , b_{fit} , and c_{fit} . The input power P_{in} into the single components is a function depending on the requested output power P_{out} [8]. $P_{in,mes}$ stems from measurement data from our Hardware-in-the-Loop (HiL)-Simulator [18] where detailed non-linear powertrain models, that are based on real-world measurement data from the Roborace cars, are implemented. The index i denotes a counter variable in the range $[1 \dots N]$.

Fig. 3 displays a polynomial fit to simulated data of an electric machine. The probability distributions of data on both axis indicate that mainly max- or minimal power is requested by the racecar. Therefore, the parabolic fit, showing high accuracy at these points, results in low MSEs. These are $e_{MS,fit,M} = 3.19\%$ for the electric machine and $e_{MS,fit,I} = 4.16\%$ for the inverter. The diagonal indicates 100 % efficiency.

We use an open circuit model to describe the internal battery power [19, p. 51] $P_{in,B}$,

$$P_{in,B}(P_{out,B}) = \frac{U_{OCV}^2}{2R_i} - U_{OCV} \frac{\sqrt{U_{OCV}^2 - 4P_{out,B}R_i}}{2R_i}. \quad (3)$$

The open circuit voltage is U_{OCV} and R_i is the internal battery resistance.

The component power loss $P_{los,c}$ can now be described using (1) and (3) that can easily be implemented within the numerical optimization,

$$P_{los,c} = P_{in,c} - P_{out,c}. \quad (4)$$

B. Thermal models

As introduced in Section II, the thermal model of the powertrain is split into two circuits, one cooling the electric machines $M_{l/r}$ and both inverters $I_{l/r}$ in series using the radiator R_{MI} , the other one being responsible for the battery

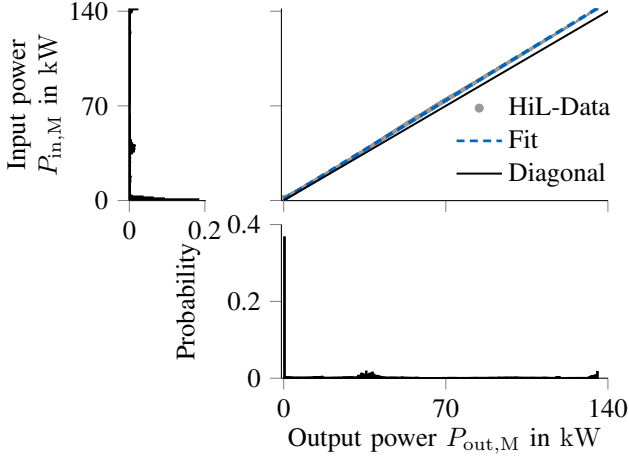


Fig. 3: Parabola fit to measurement data to deduce a polynomial expression of the electric machine's efficiency.

temperature T_B leveraging radiator R_B (Fig. 2). Power losses (4) from the electric components c are directly fed into the thermal circuits.

In the following, the ODEs describing the powertrain thermodynamics, i.e., the heat transfer from the powertrain components to the cooling liquids, are deduced. In general, the product of the thermal heat capacities C and the temperature gradients $\frac{dT}{dt}$ equal loss P_{los} and cooling power P_{col} for electric machines, inverters and battery:

$$\begin{aligned} C_M \frac{dT_M}{dt} &= P_{\text{los},M} - \frac{T_M - T_{M,\infty}}{R_M} = \\ &= P_{\text{los},M} - \underbrace{\frac{2T_M - (T_{F1,M} + T_{F1,R_{MI}})}{2R_M}}_{P_{\text{col},M}} \end{aligned} \quad (5)$$

$$C_I \frac{dT_I}{dt} = P_{\text{los},I} - \underbrace{\frac{2T_I - (T_{F1} + T_{F1,M})}{2R_I}}_{P_{\text{col},I}} \quad (6)$$

$$C_B \frac{dT_B}{dt} = P_{\text{los},B} - \underbrace{\frac{T_B - T_{F2}}{R_B}}_{P_{\text{col},B}}. \quad (7)$$

Here and in the following, $T_{F1} = T_{F1,I}$. The symbol $T_{M,\infty}$ denotes the temperature of the surroundings of the specific component M . This temperature can be assumed to be equal to the mean value of the inflowing and effluent cooling liquid temperature [20].

To describe the absorbed energy by the coolant fluid from both inverters the following formulation is used:

$$2 \frac{T_I - T_{I,\infty}}{R_I} = \dot{m}_{F1} c_F (T_{F1,M} - T_{F1}), \quad (8)$$

where \dot{m}_{F1} describes the coolant mass flow through both inverters and c_F the specific heat capacity of the coolant fluid. Using $T_{I,\infty} = \frac{1}{2} (T_{F1} + T_{F1,M})$, the following equations can be deduced to explicitly describe the temperatures of the cooling liquid entering electric machines as well as the

radiator R_{MI} :

$$T_{F1,M} = \frac{T_{F1} (\dot{m}_{F1} c_F R_I - 1) + 2T_I}{1 + \dot{m}_{F1} c_F R_I} \quad (9)$$

$$T_{F1,R_{MI}} = \frac{T_{F1} (2\dot{m}_{F1} c_F R_{R_{MI}} + 1) - 2T_{\text{env}}}{2\dot{m}_{F1} c_F R_{R_{MI}} - 1}. \quad (10)$$

We can formulate the gradients of T_{F1} and T_{F2} using the cooling power of the powertrain components P_{col} as well as the temperature differences to the environment T_{env} ,

$$\begin{aligned} C_{F1} \frac{dT_{F1}}{dt} &= 2P_{\text{col},M} + \\ &\quad + 2P_{\text{col},I} - \\ &\quad - \frac{1}{R_{R_{MI}}} \left(\frac{T_{F1,R_{MI}} + T_{F1}}{2} - T_{\text{env}} \right) \end{aligned} \quad (11)$$

$$C_{F2} \frac{dT_{F2}}{dt} = P_{\text{col},B} - \frac{T_{F2} - T_{\text{env}}}{R_{R_B}}. \quad (12)$$

The thermal resistance of the motor model R_M can be written as a combination of two thermal resistances $R_{1/2}$ in parallel as the heat transfer acts from the air gap to both directions, the environment as well as its shaft (Fig. 4). For this model we make use of [21] that describes the stator winding temperature T_W as highest and most critical. $T_{F1,M} = \frac{1}{2} (T_{F1,M} + T_{F1,R_{MI}})$ denotes the mean temperature of the cooling liquid through the electric machine. Therefore,

$$R_M = \frac{R_1 R_2}{R_1 + R_2}, \quad (13)$$

with

$$R_1 = \frac{\ln \frac{r_4}{r_3}}{2\pi L k_{\text{iro}}} + \frac{1}{2\pi r_4 L h_f} \quad (14)$$

$$R_2 = \frac{\ln \frac{r_2}{r_1}}{2\pi L k_{\text{iro}}} + \frac{1}{4\pi L k_{\text{iro}}} + \frac{1}{2\pi r_3 L h_g}. \quad (15)$$

Fig. 4 indicates the geometry of the electric machine. The first term in resistance R_1 takes into account conduction of the stator where L denotes its length and k_{iro} the thermal conductivity of iron. The second term describes the convective heat flux between the stator and the cooling liquid with h_f being the liquid's convective heat flux coefficient that can be assumed constant [22, p. 11]. Resistance R_2 consists of the thermal conductivity of the rotor and shaft [16] as well as the convection into the air gap with the respective heat flux coefficient h_g .

The thermal resistance of the inverter is assumed to be

$$R_I = \frac{1}{A_I h_I}, \quad (16)$$

as well as for the battery [20]

$$R_B = \frac{1}{A_B h_B}, \quad (17)$$

and the radiators

$$R_{R_{MI/B}} = \frac{1}{A_{R_{MI/B}} h_{R_{MI/B}}}. \quad (18)$$

Here, A denotes the surface used for the heat exchange, h again represents heat flux coefficients.

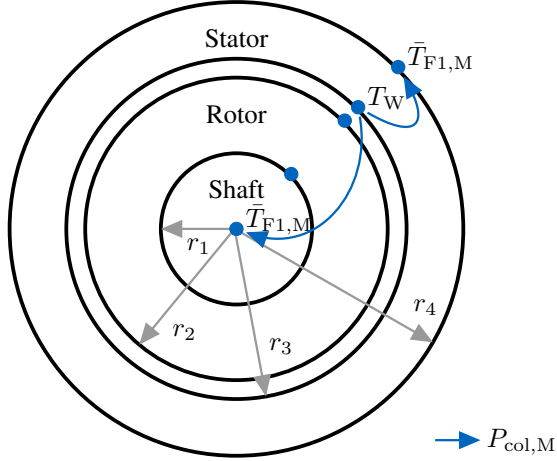


Fig. 4: Thermal resistance model of the electric machine.

C. Optimization problem

The OCP transformed into an NLP with equality and inequality constraints h_i and g_j has the form [23, p. 478], [24, p. 127]

$$\min l(\mathbf{x}) = \int_0^{S_\Sigma} \frac{dt}{ds} ds = \int_0^{S_\Sigma} \frac{1 - n\kappa}{v \cos(\xi + \beta)} ds \quad (19)$$

$$s.t. \quad \frac{d\mathbf{x}}{ds} = f(\mathbf{x}(s), \mathbf{u}(s)) \quad (20)$$

$$h_i = 0 \quad (21)$$

$$g_j \leq 0 \quad (22)$$

with $i = 1, \dots, m$ and $j = 1, \dots, r$. The independent variable is s , the distance along the reference line, κ denotes the curvature profile of the race track. The objective is $l(\mathbf{x})$, defined as the integral over the lethargy $\frac{dt}{ds}$ [8] being minimized over the entire racing distance S_Σ . The lethargy can be interpreted as the time taken to travel a distance of 1 m.

The state vector $\mathbf{x}(s)$ within the OCP is defined as

$$\mathbf{x}(s) = \left(\underbrace{v \ \beta \ \psi \ n \ \xi}_{\text{Driving Dynamics}} \ \underbrace{T_M \ T_I \ T_B \ T_{F1} \ T_{F2}}_{\text{Thermodynamics}} \right)^T, \quad (23)$$

consisting of the optimization variables needed to express the thermodynamics as introduced in Section II-B as well as the variables defining the driving dynamics. These variables are the velocity v on the raceline, the side slip angle β , the yaw angle ψ , the lateral distance to the reference line n , and ξ as the relative angle of the vehicle's longitudinal axis to the tangent on the reference line. For a detailed description of the driving dynamics as well as their first-order ODEs and constraints stemming from a nonlinear double track model, we refer to our previous works [5], [25], as we focus on the thermodynamical side within this paper.

The box constraints that are translated into inequality constraints for the thermodynamical state variables are

$$T_{c,\min} \leq T_c \leq T_{c,\max}, \quad (24)$$

with every component's allowed operating temperature range defining the lower $T_{c,\min}$ and upper boundaries $T_{c,\max}$. The input vector has the form

$$\mathbf{u}(s) = (F_d \ F_b \ \delta \ \gamma)^T, \quad (25)$$

containing driving and braking force F_d/F_b , the steering angle δ , and the wheel load transfer γ as artificial control variable.

III. RESULTS

The results were calculated using an i7-7820HQ CPU and 16 GB of memory. The NLP was solved with the primal-dual interior-point method IPOPT interfaced by CasADi [26] using a direct collocation transcription. The execution time of the solver for the NLP for two race laps was approximately 2.5 min. The discretization step size varied along the race-track. In curves, a finer mesh was implemented to allow for a better description of the rapidly changing variables and their gradients leading to a step size of $\Delta s = 3$ m. On the straight parts, a coarser mesh of $\Delta s = 9$ m was sufficient to reach high numerical precision in combination with small computation times. In total, approx. $44 \cdot 10^3$ decision variables and $50 \cdot 10^3$ constraints were present.

Two minimum race-time control strategies for a race, consisting of two laps, can be seen in Fig. 6. Two different cases were considered: In case “cold” (−), the initial temperatures of all the powertrain components $T_{c,0,-}$ equaled the environment temperature T_{env} . In case “hot” (+), the initial component temperatures $T_{c,0,+}$ were set to the values given in Table I.

TABLE I: Initial temperature values $T_{c,0}$ of powertrain components.

	$T_{M,0}$	$T_{I,0}$	$T_{B,0}$	$T_{F1,0}$	$T_{F2,0}$
	in °C				
“cold” (−)	30	30	30	30	30
“hot” (+)	100	70	48	55	40

In case “cold”, none of the components c reached their maximum allowed temperature. Therefore, the maximum vehicle power of $P_\Sigma = Fv$ of 270 kW could be requested at all times when allowed by the driving dynamics as displayed in the last plot. The maximum physically achievable velocity of approx. 220 km h^{-1} for this vehicle on the Montebianco race-track resulted on the straights. The battery temperature T_B remained far below the limit of $T_{B,\max} = 50^\circ\text{C}$.

Case “hot” shows the necessity and performance of the developed control-strategy. Here, the initial component temperatures $T_{c,0,+}$ were set to a valid combination of reasonable values (Table I) that can occur during a race. The optimization's initial battery temperature $T_{B,0,+}$ almost equaled $T_{B,\max}$. The race-strategy then was adapted to the given conditions to reach $T_{B,\max}$ exactly when crossing the finish line at $s = 4.73 \text{ km}$ to avoid a safety stop during the

race. This was achieved by augmented phases of lift and coast in comparison with the race-strategy for case “cold”: As the requested power $P_{\Sigma,+}$ shows, the vehicle braked later before curves. Additionally, the requested power $P_{\Sigma,+}$ slowly decreased on the straights. When the driving resistances could not be overcome by $P_{\Sigma,+}$, the vehicle’s velocity v_+ decreased till the entry of the next curve. Therefore, the breaks could be applied late. Still, acceleration phases overlapped in both strategies, even if they ended in different maximum velocities v . The requested power maxima differed in their absolute values. The influence on the vehicle speed v_+ in case “hot” is evident: Physically, maximum velocity was never reached and mean acceleration as well as deceleration occurred less aggressively, meaning the velocity’s gradients were decreased.

The coolant fluid temperature $T_{F2,+}$ reached an equilibrium at the end of the optimization horizon since only as much heat was allowed to be released internally by the battery as the coolant fluid could dissipate. Coolant circuit F1 could be neglected in this case. Machine and inverter temperatures $T_{M,+}$ and $T_{I,+}$ did not reach their limits.

Another important point is the difference in the race paths to be driven in both cases (Fig. 5). In case “hot” velocity v_+ in curve 4 (marked) was higher. This per se had a positive influence on the lap time. Nevertheless, the higher curve speed v_+ required the path to change slightly within and immediately after this turn. Since the combined tire usage was already at the limit here, the race-path radius in case “hot” increased. By this, its curvature decreased and the higher speed v_+ could feasibly be driven. Nevertheless, the decreased acceleration after turn 4 led to a diminished increase of the powertrain temperatures.

The total race times cumulated over the two laps were 142.12 s in case “cold” and 149.59 s in case “hot”.

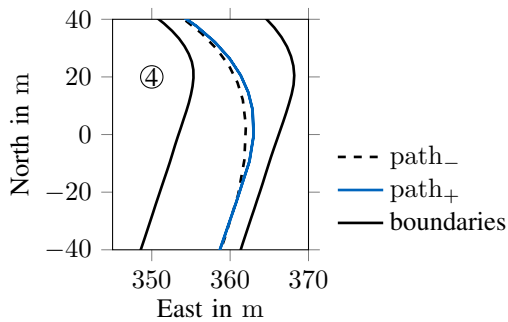


Fig. 5: Race paths for case “cold” and “hot”.

IV. CONCLUSION & OUTLOOK

In the next Roborace season, the methods presented in this publication will be applied to the racecar. On the one hand, the available energy can then be used as effectively as possible. On the other hand, the powertrain components can be exploited as much as possible without losing race time. Additionally, powertrain losses and component temperatures can then be compared with measurement data we receive

when driving the proposed global race lines that were calculated considering the thermodynamical influence.

Furthermore, an additional optimization will be implemented that allows for the mentioned online re-planning of the race-strategy in the presence of disturbances. With the help of the results in this publication this simplified online optimization can be realized.

Along with these improvements the loss-models will be replaced by physically more detailed descriptions of the powertrain components.

CONTRIBUTIONS

T. H. initiated the idea of the paper and contributed significantly to the concept, modeling, and results. F. P. modeled the powertrain thermodynamics in his Masters thesis. J. B. contributed to the whole concept of the paper. M. L. provided a significant contribution to the concept of the research project. He revised the paper critically for important intellectual content. M. L. gave final approval for the publication of this version and is in agreement with all aspects of the work. As a guarantor, he accepts responsibility for the overall integrity of this paper.

ACKNOWLEDGMENT

We would like to thank the Roborace team for giving us the opportunity to work with them and for the use of their vehicles for our research project. Special thanks to Ollie Walsh for generously sharing measurement data. We would also like to thank the Bavarian Research Foundation (Bayerische Forschungsförderung) for funding us in connection with the “rAIcing” research project.

REFERENCES

- [1] J. Betz, A. Wischnewski, Heilmeyer, A., Nobis, F., T. Stahl, L. Hermansdorfer, T. Herrmann, and M. Lienkamp, “A Software Architecture for the Dynamic Path Planning of an Autonomous Racecar at the Limits of Handling,” in *8th IEEE International Conference on Connected Vehicles and Expo (ICCVE 2019)*. IEEE, In Press, 2019.
- [2] J. Betz, A. Wischnewski, A. Heilmeyer, F. Nobis, T. Stahl, L. Hermansdorfer, B. Lohmann, and M. Lienkamp, “What can we learn from autonomous level-5 motorsport?” in *9th International Munich Chassis Symposium 2018*, ser. Proceedings, P. Pfeffer, Ed. Wiesbaden: Springer Fachmedien Wiesbaden, 2019, pp. 123–146.
- [3] J. Betz, A. Wischnewski, A. Heilmeyer, F. Nobis, T. Stahl, L. Hermansdorfer, and M. Lienkamp, “A Software Architecture for an Autonomous Racecar,” in *2019 IEEE 89th Vehicular Technology Conference (VTC2019-Spring)*. IEEE, 2019, pp. 1–6.
- [4] Chair of Automotive Technology, “Autonomous Driving Control Software of TUM Roborace,” 2019. [Online]. Available: https://github.com/TUMFTM/veh_passenger
- [5] T. Herrmann, F. Christ, J. Betz, and M. Lienkamp, “Energy Management Strategy for an Autonomous Electric Racecar using Optimal Control,” in *2019 IEEE 22th International Conference on Intelligent Transportation Systems (ITSC)*. Piscataway, NJ: IEEE, 2019.
- [6] J. h. Jeon, R. V. Cowlagi, S. C. Peters, S. Karaman, E. Frazzoli, P. Tsotras, and K. Iagnemma, “Optimal Motion Planning with the Half-Car Dynamical Model for Autonomous High-Speed Driving,” in *American Control Conference (ACC)*. Piscataway, NJ: IEEE, 2013, pp. 188–193.
- [7] A. Carvalho, Y. Gao, A. Gray, E. Tseng, and F. Borrelli, “Predictive Control of an Autonomous Ground Vehicle using an Iterative Linearization Approach,” in *16th International IEEE Conference on Intelligent Transportation Systems (ITSC)*, 2013. Piscataway, NJ: IEEE, 2013.

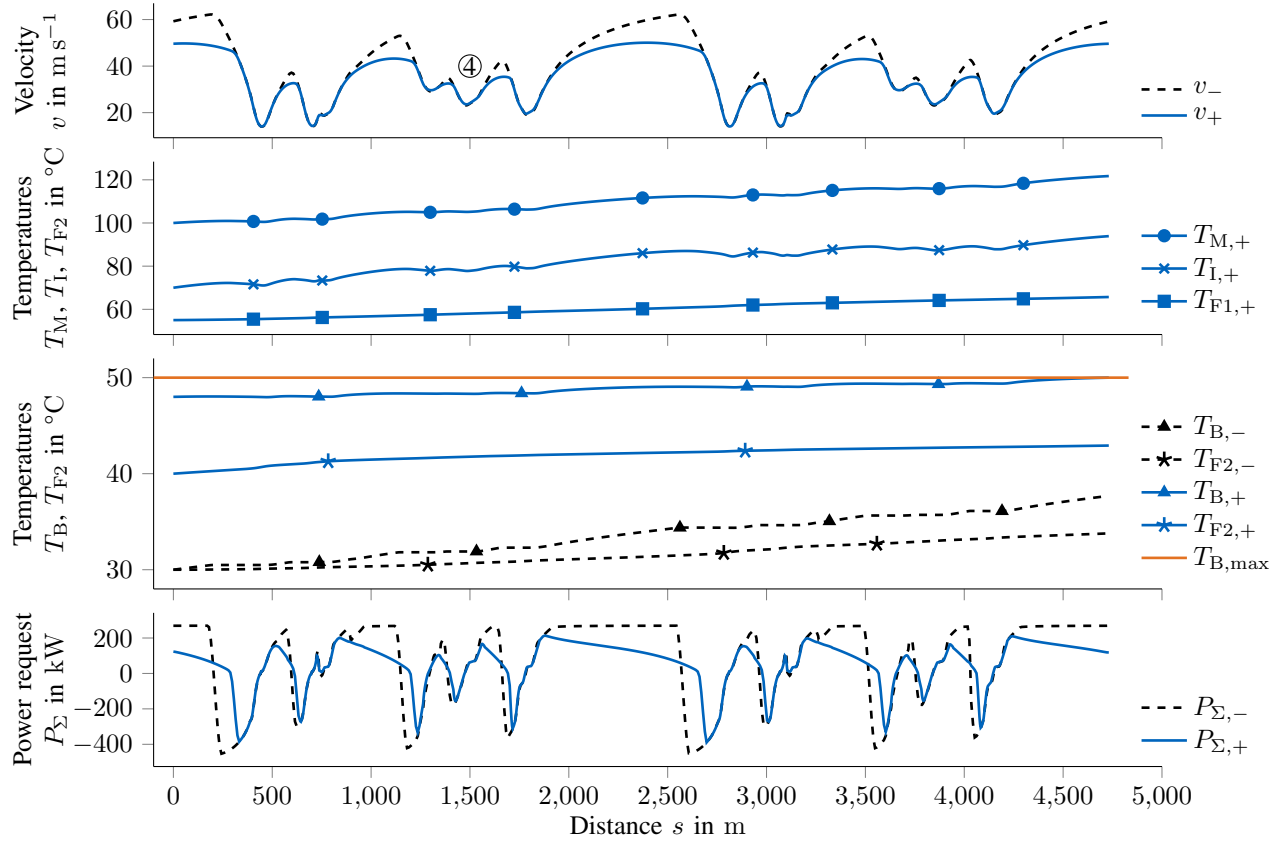


Fig. 6: Optimal race strategies for two laps on the Monteblanco race circuit showing velocity v , power request P_{Σ} and component temperatures T_c .

- [8] S. Ebbesen, M. Salazar, P. Elbert, C. Bussi, and C. H. Onder, "Time-optimal Control Strategies for a Hybrid Electric Race Car," *IEEE Transactions on Control Systems Technology*, vol. 26, no. 1, pp. 233–247, 2018.
- [9] C. Kirches, S. Sager, H. G. Bock, and J. P. Schlöder, "Time-optimal control of automobile test drives with gear shifts," *Optimal Control Applications and Methods*, vol. 31, no. 2, pp. 137–153, 2010.
- [10] D. J. N. Limebeer and G. Perantoni, "Optimal Control of a Formula One Car on a Three-Dimensional Track—Part 2: Optimal Control," *Journal of Dynamic Systems, Measurement, and Control*, vol. 137, no. 5, p. 051019, 2015.
- [11] M. Imani Masouleh and D. J. N. Limebeer, "Optimizing the Aero-Suspension Interactions in a Formula One Car," *IEEE Transactions on Control Systems Technology*, vol. 24, no. 3, pp. 912–927, 2016.
- [12] M. Salazar, P. Elbert, S. Ebbesen, C. Bussi, and C. H. Onder, "Time-optimal Control Policy for a Hybrid Electric Race Car," *IEEE Transactions on Control Systems Technology*, vol. 25, no. 6, pp. 1921–1934, 2017.
- [13] D.-m. Wu, Y. Li, C.-q. Du, H.-t. Ding, Y. Li, X.-b. Yang, and X.-y. Lu, "Fast velocity trajectory planning and control algorithm of intelligent 4WD electric vehicle for energy saving using time-based MPC," *IET Intelligent Transport Systems*, vol. 13, no. 1, pp. 153–159, 2019.
- [14] Roborace, "Roborace Ltd." 2018. [Online]. Available: <https://roborace.com/>
- [15] J. Schuetzhold and W. Hofmann, "Analysis of the Temperature Dependence of Losses in Electrical Machines," in *IEEE Energy Conversion Congress and Exposition (ECCE)*, 2013. Piscataway, NJ: IEEE, 2013, pp. 3159–3165.
- [16] K. Li, S. Wang, and J. P. Sullivan, "A novel thermal network for the maximum temperature-rise of hollow cylinder," *Applied Thermal Engineering*, vol. 52, no. 1, pp. 198–208, 2013.
- [17] T. Stahl, A. Wischnewski, J. Betz, and M. Lienkamp, "Multilayer Graph-Based Trajectory Planning for Race Vehicles in Dynamic Scenarios," in *2019 IEEE 22th International Conference on Intelligent Transportation Systems (ITSC)*. Piscataway, NJ: IEEE, 2019.
- [18] T. Herrmann and M. Luethy, "A Real-Time Simulation Environment for Autonomous Vehicles in Highly Dynamic Driving Scenarios," 2019. [Online]. Available: <https://de.mathworks.com/videos/a-real-time-simulation-environment-for-autonomous-vehicles-in-highly-dynamic-driving-scenarios-1558698299193.html>
- [19] A. Sciarretta and A. Vahidi, *Energy-Efficient Driving of Road Vehicles: Toward Cooperative, Connected, and Automated Mobility*, 1st ed., ser. Lecture Notes in Intelligent Transportation and Infrastructure. Cham: Springer International Publishing and Springer, 2020.
- [20] T. Han, B. Khalighi, E. C. Yen, and S. Kaushik, "Li-Ion Battery Pack Thermal Management: Liquid Versus Air Cooling," *Journal of Thermal Science and Engineering Applications*, vol. 11, no. 2, p. 5115, 2019.
- [21] A. M. EL-Refai, N. C. Harris, T. M. Jahns, and K. M. Rahman, "Thermal Analysis of Multibarrier Interior PM Synchronous Machine Using Lumped Parameter Model," *IEEE Transactions on Energy Conversion*, vol. 19, no. 2, pp. 303–309, 2004.
- [22] F. P. Incropera, D. P. DeWitt, T. L. Bergman, and A. S. Lavine, *Fundamentals of heat and mass transfer*, 6th ed. Hoboken, NJ: Wiley, 2007.
- [23] D. P. Bertsekas, *Dynamic programming and optimal control*, 4th ed., ser. Athena scientific optimization and computation series. Belmont, Mass.: Athena Scientific, 2016, vol. 3.
- [24] S. P. Boyd and L. Vandenberghe, *Convex optimization*, ser. Safari Tech Books Online. Cambridge, UK and New York: Cambridge University Press, 2004.
- [25] F. Christ, A. Wischnewski, A. Heilmeier, and B. Lohmann, "Time-optimal trajectory planning for a race car considering variable tyre-road friction coefficients," *Vehicle System Dynamics*, vol. 3, no. 1, pp. 1–25, 2019.
- [26] J. A. E. Andersson, J. Gillis, and G. Horn, "CasADi – A software framework for nonlinear optimization and optimal control," *Mathematical Programming Computation*, 2018.